Full-Duplex Antenna Subsystem for Microwave Radio Links

Prathap Valale Prasannakumar, *Student Member, IEEE*, Mohamed A. Elmansouri, *Senior Member, IEEE*, Ljubodrag Boskovic, and Dejan S. Filipovic, *Senior Member, IEEE*

***Abstract*—The design of an in-band full-duplex antenna subsystem for a point-to-point microwave link is outlined. High isolation between the transmitter and receiver is achieved through the balanced-circulator approach. In the proposed approach, reflected signals from the antenna and the coupled/leaked signals from the circulators are canceled at the RX port of the beamforming network (BFN) leading to high system isolation. The utilized BFN consists of two 90° hybrids and two circulators. The realized full-duplex antenna is a circularly-polarized parabolic reflector antenna having gain > 20 dB, and return loss > 10 dB. System isolation > 30 dB is achieved. The impact of cross-polarization and the physical asymmetries on the system isolation is also discussed. Moreover, analog signal cancelation technique is applied to compensate imbalances and further improve the system isolation.**

***Index Terms*—Full-duplex, isolation, tactical radio relay.**

I. Introduction

THE increase in the number of wireless devices has created demand for higher bandwidth channels. Hence, there is a need for efficient frequency spectrum utilization. In-band full-duplex systems, which are also referred as simultaneous transmit and receive (STAR) systems, are capable of transmitting at the same time and frequency without any multiplexing, thereby, improving the system throughput and spectral efficiency. However, isolation between the transmitter (TX) and receiver (RX) on the order of > 110 dB is required for the practical realization of a STAR system. The required isolation is typically achieved by minimizing the self-interference between TX and RX at different layers in antenna, analog and digital domains [1].

An in-band full-duplex antenna sub-system for microwave point-to-point radio link is discussed in this work. In the proposed approach, high isolation between TX and RX is achieved by rerouting the coupled, leaked, and reflected signals, through a beamforming network (BFN) consisting of hybrids and circulators [2]-[3]. A self-supporting axis symmetric parabolic reflector antenna with coaxial cavity antenna as a feed is designed. The fabricated system achieves average measured isolation of 30 dB, where COTS components are used in the BFN. The impact of surface roughness, and cross-pol level of the antenna on system isolation is presented. Additionally, an analog cancelation network is employed to further improve the isolation of the overall (analog to this point) system [4]. Digital baseband cancellation is needed to achieve >110dB of isolation.

The authors are with the Department of Electrical, Computer, and Energy Engineering, University of Colorado at Boulder, Boulder, CO 80309 USA (e-mail: {Prathap.Valaleprasannakumar, mohamed.elmansouri, Ljubodrag.boskovic, dejan.filipovic} @colorado.edu).

II. Full-Duplex Realization

The proposed monostatic full-duplex system is realized using a simple BFN composed of two 90° hybrids and two circulators. The antenna is dual-linearly polarized and the proposed excitation through the utilized BFN will enable dual TX/RX circularly-polarized operation. The schematic and the signal flow in the BFN are shown in the Fig. 1. High isolation between the TX and RX is achieved by carefully rerouting the coupled, leaked and reflected signals such that these signals cancel at the RX port. Specifically, the signal to be transmitted (or TX signal) is fed to the input of the 90° Hybrid 1, thus the signals at the output are of equal magnitude and quadrature phase. Further, the signals from the output of 90° Hybrid 1 are routed through the paths I and II. These voltages pass through the circulators 1 and 2, before reaching the antenna input terminals. The reflected signals (1) and (2) from the antenna and the coupled/leaked from the circulators are connected to the input of the 90° Hybrid 2. Herein, S_{21}^{C1} and S_{31}^{C1} are S_{21} and S_{31} of circulator I, respectively. Similarly, S_{21}^{C2} and S_{31}^{C2} are S_{21} and S_{31} of circulator II, respectively. $|\Gamma_1|$, and $|\Gamma_2|$ are the reflections from the ports 1 and 2 of the antenna. The signal from path I (1) undergoes another 90° phase shift after passing through the hybrid 2, thereby resulting in the total cancelation of the reflected and leaked signals at the RX port. This leads to theoretically infinite isolation between TX and RX. The reflected signals are combined in phase at the port P4 of the hybrid 2 (i.e. RX hybrid), which is terminated with matched load.

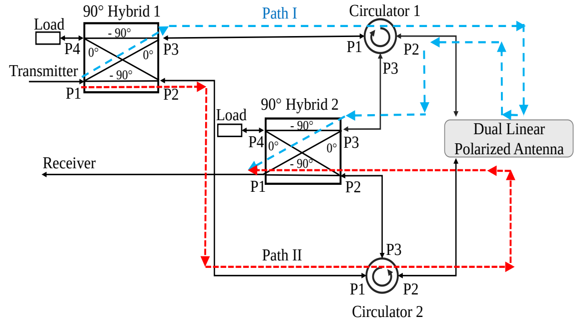

Fig. 1. Schematic and signal flow of the proposed high directivity, reflector-based full-duplex antenna system.

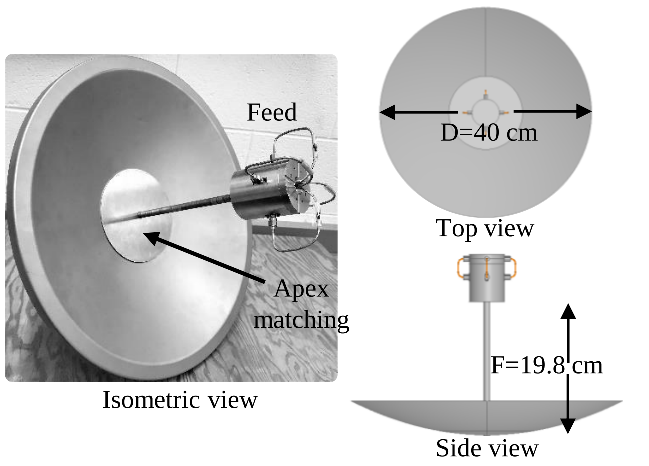

Fig. 2. Picture of the fabricated antenna and its CAD model along with corresponding dimensions.

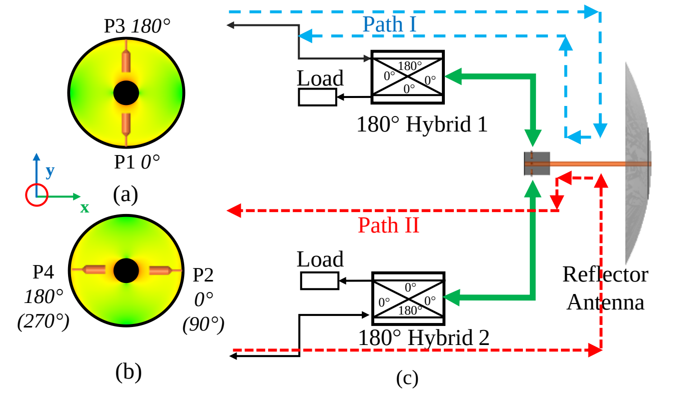

Fig. 3. Electric field distribution at the aperture of the coaxial cavity antenna feed for the TE_{11} mode in (a) y-direction, and (b) x-direction. (c) Illustration of the BFN used to realize the TE_{11} mode.

$$|\Gamma_1|\frac{-1}{2}e^{j\varphi}\cdot S_{21}^{C1}\cdot S_{32}^{C1}. \tag{1}$$

$$|\Gamma_2|\frac{1}{2}e^{j\varphi}\cdot S_{21}^{C2}\cdot S_{32}^{C2}. \tag{2}$$

However, the asymmetries in antenna structure or the imbalances in the BFN will create amplitude and phase imbalances between signals from the path I and II, thereby leading to the finite isolation.

III. Microwave Radio Links

A. *Antenna Design and Performance*

The axis-symmetric parabolic reflector antenna along with feed and the dimensions are shown in Fig. 2. The antenna is designed to operate over C-band, i.e. from 4 to 8 GHz. Axis-symmetric reflector configuration is employed over the offset configuration in order to avoid the asymmetry in the antenna geometry and in the radiation patterns. The reflector has diameter and focal length of 40 cm and 19.8 cm, respectively; that is F/D = 0.495. The reflector is fed by a coaxial cavity antenna which has phase center variation < 5

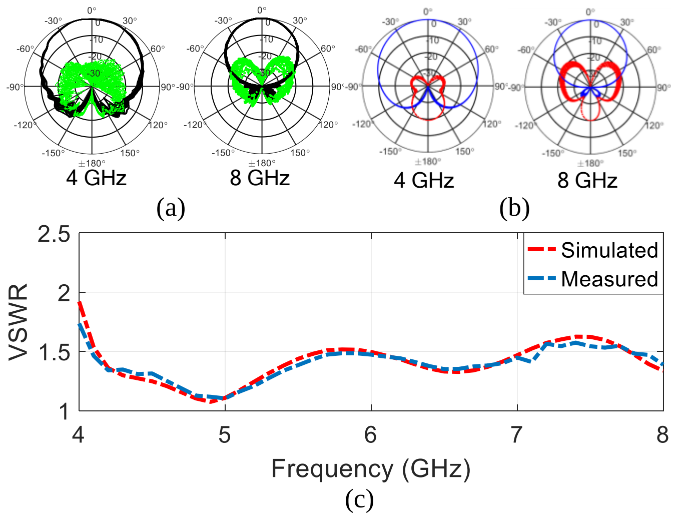

Fig. 4. (a) Measured (black-LHCP, green-RHCP) and (b) simulated (blue-LHCP, red-RHCP) radiation patterns. and (c) measured and simulated VSWR of the coaxial cavity antenna.

% for θ = ± 53°over the operating band [5]. Operation of the coaxial cavity antenna is analogous to an open-ended coaxial waveguide. Two probes, oriented along y-axis is fed with 180° phase difference to excite the TE_{11} (vertical polarization) mode of the cavity, as shown in Fig. 3(a). Similarly, another set of probes, oriented along the x-axis (see Fig. 3(b)) with 180° phase difference is used to excite the horizontal polarization. The BFN required for dual linear polarization is shown in Fig. 3(c). Further, the 90° hybrids in Fig. 1 are used to realize dual CP operation. The impedance match of the coaxial cavity antenna is improved by shaping the exciting probes (see Figs. 3(a) and (b)), and by selecting the proper ratio of inner to outer conductor diameter, *b*, and *a*, respectively [6]. Further, the pattern symmetry in E and H planes is dependent on the b/a ratio. Hence, as a trade-off between pattern symmetry and impedance match, b/a=0.23 is selected for the prototype design. Thus, the resulting antenna has symmetric radiation patterns (Figs. 4(a), and (b)), axial ratio (AR) < 3 dB up to θ = ± 30°, and VSWR < 2 over an octave of bandwidth, as shown in Fig. 4(c). The VSWR of the antenna is lower than that in [7].

Conventionally, the feed of an axis-symmetric reflector is supported by 3 or 4 struts, which can degrade the radiation patterns by increasing the side lobe level (SLL), and decreasing the gain [8]. Therefore, a self-supporting configuration is proposed in this work, where the inner conductor of the coaxial cavity antenna (feed) is extended up to the apex of the reflector. Hence, the inner conductor also functions as the support for the feed, as shown in Fig. 2. The extension of the inner conductor has less influence on the impedance match since the resulting reflector antenna maintains VSWR < 2 [5]. Moreover, the proposed reflector antenna has symmetric radiation patterns with low cross-pol and SLL < -10 dB, see Fig. 5(a). Additionally, the directivity is > 20 dBic over the band, and the measurements are in good agreement with the simulation results, as shown in Fig. 5 (b).

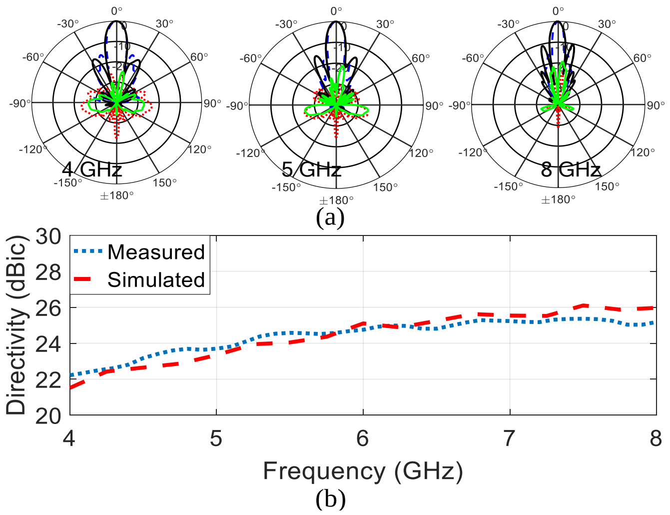

Fig. 5. (a) Measured (black-LHCP, green-RHCP) and simulated radiation patterns (blue-LHCP, red-RHCP), and (b) directivity of the reflector antenna.

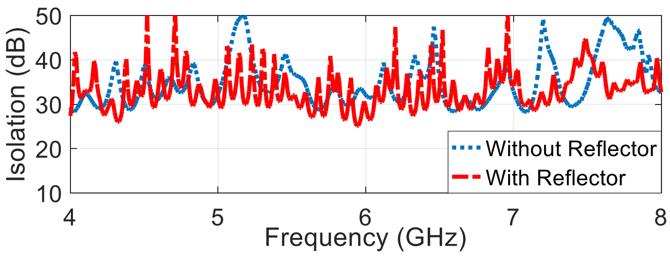

Fig. 6. Measured isolation of the proposed system with and without reflector.

B. System Isolation

The reflector antenna which design is described above is integrated with the BFN in Fig. 1 to realize the proposed monostatic full-duplex antenna. System isolation > 30 dB is achieved with and without the reflector using the proposed configuration. Lower isolation in the measurement is mainly due to the imbalances in the BFN components. Nonetheless, the isolation achieved is ~ 10 dB higher than the isolation of the used circulators. The COTS 90° hybrids having ±0.5 dB and ±3°, amplitude and phase imbalances, respectively are used. Similarly, the 180° hybrids in BFN have ±0.6 dB and ±10°, amplitude and phase imbalances, respectively. In addition, the circulators with 20 dB isolation, 0.35 dB insertion loss, and VSWR < 1.25 are used.

C. Impact of cross-pol and asymmetries

The proposed approach relies on the symmetry in the antenna geometry and BFN for total signal cancelation, as mentioned in Section II. The impact of the reflector on the measured system isolation is insignificant (Fig. 6), since the geometry is symmetric, reflector surface is smooth, and mainly small imperfection in the geometry is overshadowed by the imbalances in BFN. However, often, large reflectors surface undergo aberrations or structural deformation over the time, and the fabrication processes can increase the roughness of the surface [9], thereby, affecting the system isolation.

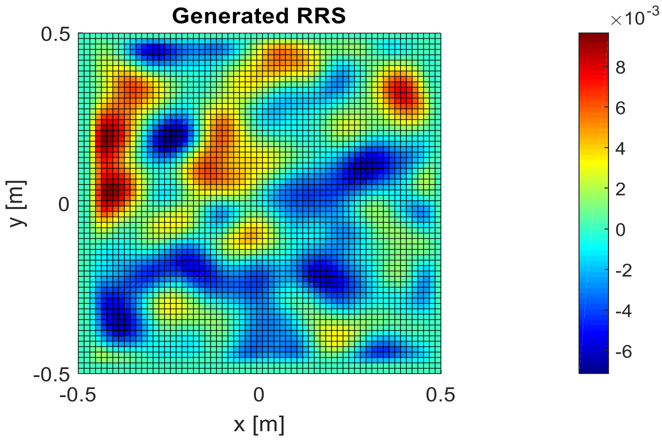

Fig. 7. Gaussian random rough surface (RRS) projected on *xy* plane.

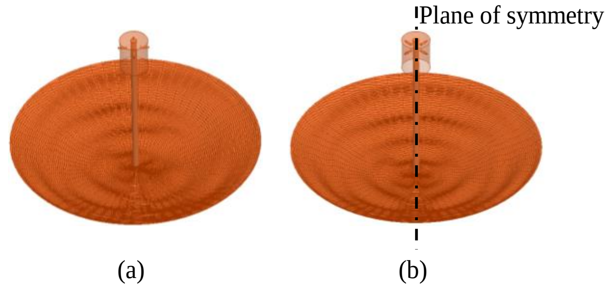

Fig. 8. CAD model of reflector antenna: (a) asymmetric rough surface, and (b) symmetric rough surface.

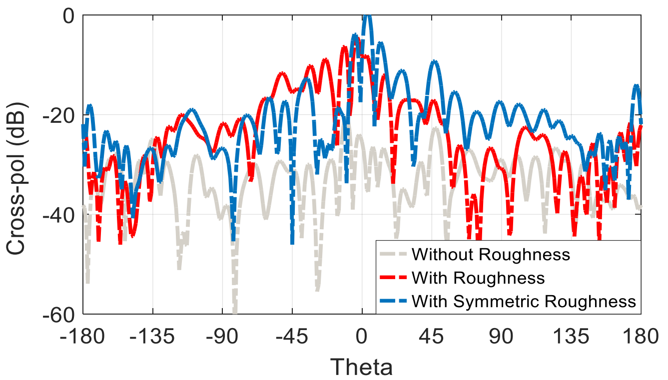

Fig. 9. Simulated cross-pol. patterns of the reflector antenna for the surface without roughness, and with symmetric and symmetric roughness, at $\phi = 0^{\circ}$.

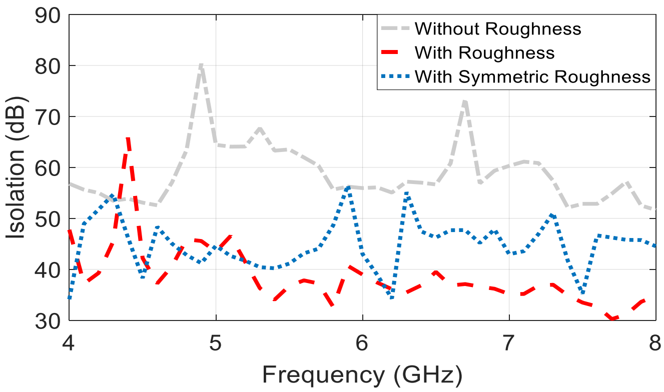

Fig. 10. Simulated isolation of the proposed system for the surface without roughness, and with symmetric and symmetric roughness. Ideal BFN is used in this analysis.

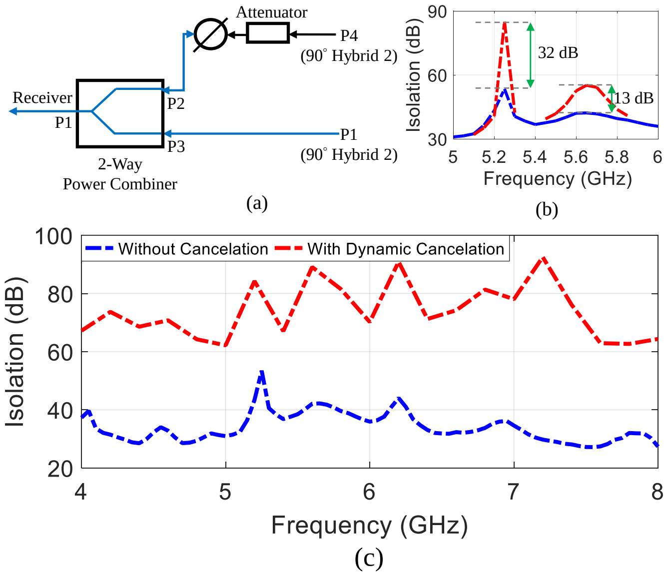

Fig. 11. (a) Analog cancelation network. Simulated isolation with cancelation (b) over narrow bandwidth, and (c) over wider bandwidth.

The roughness of the surfaces is modeled as a Gaussian distribution with correlation length comparable to wavelength and the root-mean-square (rms) height much less than the wavelength. Specifically, the surface roughness with correlation length 10 cm (1.33 λ_{4GHz}) and rms height of 0.3 cm (0.04 λ_{4GHz}) is used. The generated rough surface projected on *xy* plane is shown in Fig. 7. Three cases; smooth surface, rough surface with rms 0.3 cm, and a symmetric rough surface (see Fig. 8) are considered herein to analyze the impact of symmetry on the cross-polarized level as well as system isolation. The corresponding cross-polarized pattern of the reflector antenna (for linear polarization) at $\phi = 0^{\circ}$ is shown in Fig. 9, where the increase in cross-pol level with increasing roughness can be clearly observed. Further, the increase in cross-pol has deteriorated the system isolation as shown in Fig. 10. However, the imbalances created in antenna ports are higher in case of the asymmetric rough surface, when compared to the symmetric rough surface. Hence, the deterioration in isolation with the asymmetric case is higher than in the symmetric case. Thus, the results in Fig. 10 indicate that the physical imperfections could also deteriorate the system isolation. However, if the imperfections are symmetric the influence on the system isolation can be reduced, as shown in Fig, 10.

D. Isolation Improvement Techniques

Furthermore, the isolation of the system can be increased by using analog cancelation technique [4], where the signals from ports 4 and 1 of 90° Hybrid 2 are combined to compensate for the imbalances in the BFN components, as shown in Fig. 11 (a). The isolation can be increased up to 32 dB over a narrow bandwidth using this cancelation technique, as illustrated in Fig. 11(b). In addition, the improvement in the isolation over a wider bandwidth can be achieved by employing a dynamic cancelation network, as shown in the simulated results in Fig. 11 (c). The measured S-parameters of the BFN components, and the simulated antenna are used in the circuit simulator (AWR Microwave Office) to realize the circuit and results in Fig. 11.

IV. Conclusion

The design of high directivity, monostatic, circularly-polarized reflector antenna is discussed. The balanced-circulator approach is used to achieve high antenna level isolation between the TX and RX. Measured isolation > 30 dB is achieved. It is shown that the influence of reflector on the proposed STAR approach is minimal. However, physical asymmetries could deteriorate the isolation. Also, it is demonstrated that the imbalances in the BFN can be compensated over narrow bandwidth using a simple analog cancelation technique. To achieve >110dB of isolation required for the entire STAR system, the digital baseband cancellation level will need to be added.

Acknowledgment

Authors like to acknowledge the Army Research Office (ARO) and the Office of Naval Research (ONR) for funding this work, under the award numbers W911Nf-17-1-0228 and N00014-17-1-2882, respectively.

References

[1] H. Krishnaswamy *et al.*, "Full-duplex in a hand-held device — from fundamental physics to complex integrated circuits, systems and networks: An overview of the Columbia FlexICoN project," *2016 50th Asilomar Conf. on Signals, Systems and Computers*, Pacific Grove, CA, 2016, pp. 1563 – 1567.

[2] M. E. Knox, "Single antenna full duplex communications using a common carrier," *IEEE Wireless Micro. Tech. Conf.*, Cocoa Beach, FL, Apr.2012, pp.1 – 6.

[3] W. G. Lim and J. W. Yu, "Balanced circulator structure with enhanced isolation characteristics". *Microw. Opt. Tech. Lett*., vol. 50, 2008, pp. 2389 – 2391.

[4] J. Ha, M. A. Elmansouri, P. Valale Prasannakumar, and D. S. Filipovic, "Monostatic co-polarized full-duplex antenna with left- or right-hand circular polarization," in *IEEE Trans. Antennas Propag*, vol. 65, no. 10, pp. 5103-5111, Oct. 2017.

[5] P. Valale Prasannakumar, M. A. Elmansouri, and D. S. Filipovic, "Broadband monostatic simultaneous transmit and receive reflector antenna system," *2017 IEEE Int. Symp. on Antennas and Propag. (APSURSI)*, San Diego, 2017.

[6] Prathap. V Prasannakumar, M. A. Elmansouri and D. S. Filipovic, "Broadband reflector antenna with high isolation feed for full duplex applications," in *IEEE Trans. Antennas Propag*, Accepted.

[7] T. R. Holzheimer, "Applications of the coaxial cavity antenna in time and frequency", *2004 Antenna Appl. Symp.*, Allerton Park, Monticello, Illinois, Sep. 2004, pp.1 – 19.

[8] T. A. Milligan, *Modern antenna design*. Hoboken, NJ, USA: John Wiley & Sons, 2005, ch. 8.

[9] J. Ruze, "The effect of aperture errors on the antenna radiation pattern", *Nuevo Cimento Suppl.*, vol. 9, No. 3, 1952, pp. 364 – 380.